RVQ Revista Virtual de Química

Article

Rev. Virtual Quim. **2026**, *18(4)*, 454-460 – http://dx.doi.org/10.21577/1984-6835.20260005

Targeting Photosystem II: Design and Synthesis of 4,6-Diarylpyrimidin-2(1*H*)-thione Derivatives

Tendo Como Alvo o Fotossistema II: Design e Síntese de Derivados 4,6-Diarilpirimidin-2(1*H*)-tiona

Lucas C. C. Vieira,[a,*] Kettlyn A. R. T. Santos,[a] Taciane S. Pitteri,[a] Marcelo A. F. Basso,[a] Raquel S. Garralda,[a] Leonardo G. de Vasconcelos,[a] Olívia M. Sampaio[a]

[a] Universidade Federal de Mato Grosso, Institute of Chemistry, Zip Code 78060-900, Cuiabá-MT, Brasil

***E-mail:** lucas.vieira@ufmt.br

Submitted: 31 de Julho de 2025 – **Accepted:** 28 de Janeiro de 2026 – **Published online:** 10 de Fevereiro de 2026

This study describes the synthesis of 4,6-diarylpyrimidin-2(1*H*)-thione derivatives and their evaluation as potential inhibitors of photosystem II (PSII) through chlorophyll *a* fluorescence assays and molecular docking studies. Compounds 4,6-diphenyl-3,4-dihydropyrimidine-2(1*H*)-thione and 6-(4-bromophenyl)-4-phenyl-3,4-dihydropyrimidine-2(1*H*)-thione decreased the performance index on an absorption basis by 74% and 65%, respectively, and reduced electron transport per reaction center by 17% and 30% compared to the negative control. These effects demonstrate an impairment of the PSII electron transport chain. Docking simulations using the D1 protein subunit of PSII (PDB ID: 4V82) revealed that stereochemistry influences binding affinity and interaction profiles. The *S*-enantiomers formed stronger hydrogen bonds with key residues such as His215 and exhibited enhanced hydrophobic and π–π interactions within the active site. Overall, the results highlight the 4,6-diarylpyrimidin-2(1*H*)-thione scaffold as a promising lead for development of novel herbicidal agents targeting PSII, while underscoring the value of integrating molecular and physiological approaches to support future structure-based optimization.

Keywords: Chalcone; chlorophyll *a*; D1 protein; fluorescence; molecular docking; pyrimidin-2(1*H*)-thione.

1. Introduction

The search for environmentally safer and biologically effective herbicides remains a priority in agrochemical research, particularly in agrarian economies such as Brazil, where the overreliance on a limited number of herbicidal modes of action has accelerated the evolution of resistant weed species.[1] The widespread and prolonged use of classical photosystem II (PSII) inhibitors like atrazine and diuron has not only contributed to resistance development in weed populations, but also raised concerns about soil and water contamination, non-target toxicity, and persistence in ecosystems.[2] These challenges highlight the urgent need for novel herbicidal chemotypes that combine efficacy, selectivity, and reduced environmental impact.

In recent years, flavonoid-based scaffolds, especially chalcones, have garnered considerable attention in medicinal and agrochemical chemistry owing to their facile synthesis, structural tunability, and broad-spectrum biological activity.[3] Chalcones, as α,β-unsaturated carbonyl compounds, exhibit a range of bioactivities including antifungal,[4] anti-inflammatory,[5] anticancer,[6] and herbicidal effects.[7] Their electrophilic enone moiety is particularly reactive toward biological nucleophiles, making them ideal precursors for the construction of heterocyclic systems through annulation reactions.[8] Among the heterocyclic frameworks derived from chalcones, the 4,6-diarylpyrimidin-2(1*H*)-thione core has emerged as a promising pharmacophore in drug and agrochemical discovery. These molecules can be conveniently synthesized via the Biginelli multicomponent reaction or Mannich-type condensations involving chalcones and thiourea, providing rapid access to structurally diverse analogues.[9,10] The incorporation of sulfur into the pyrimidinone ring enhances the potential for hydrogen bonding and π-stacking interactions, which are critical for molecular recognition in protein-ligand binding.[11,12]

From a herbicidal perspective, 4,6-diarylpyrimidin-2(1*H*)-thiones are particularly attractive for their potential to inhibit PSII by targeting the QB-binding niche of the D1 protein, a vital site for plastoquinone reduction in the photosynthetic electron transport chain. Inhibitors that disrupt this process lead to an overaccumulation of energy within the photosystems, triggering oxidative damage and ultimately plant death. Molecular docking studies and

fluorescence-based PSII assays have proven to be reliable tools for evaluating such compounds, offering insights into binding affinity and functional inhibition.[13,14] To date, only a limited number of studies have investigated the role of stereochemistry in herbicides targeting PSII. One study demonstrated that the *R*-(+)-enantiomer of chiral chlorbufam shows up to 3.95-fold greater herbicidal activity than the *S*-(–)-form against *Echinochloa crus-galli*. Molecular docking analyses attributed this enantioselectivity to differences in binding affinity for the PSII D1 protein and to enantiomer-specific reductions in pigment content.[15]

In this context, the present study reports the design and synthesis of a series of 4,6-diarylpyrimidin-2(1*H*)-thione derivatives, their structural characterization, and a comprehensive biological evaluation of their herbicidal potential. The inhibitory activity on PSII was assessed via *in vivo* chlorophyll *a* fluorescence measurements, and molecular docking was performed to explore the binding interactions with the D1 protein of *Thermosynechococcus elongatus* (PDB ID: 4V82), providing a mechanistic rationale for their phytotoxic effects.

2. Experimental

2.1. Instruments and general information

All reagents and solvents used in the synthetic and bioassays procedures were purchased from Aldrich Chemical Co. and employed without further purification. Column chromatography was conducted using Merck silica gel (230–400 mesh), and thin-layer chromatography (TLC) was performed on Merck GF254 silica gel plates (0.25 mm thickness). TLC spots were visualized under UV light (254–360 nm), by exposure to iodine vapor, or by spraying with potassium permanganate or vanillin solutions.

Proton (^{1}H) and carbon (^{13}C) nuclear magnetic resonance (NMR) spectra were acquired on a Bruker Ascend™ 500 MHz spectrometer. Chemical shifts (δ) are reported in parts per million (ppm) relative to tetramethylsilane (TMS) as an internal standard, and coupling constants (J) are given in hertz (Hz). Signal multiplicities are denoted as singlet (s), doublet (d), double of doublet (dd), double of triplet (dt), triplet (t), and multiplet (m). Deuterated chloroform ($CDCl_3$) and dimethyl sulfoxide-d_6 (DMSO-d_6) were used as solvents for NMR measurements.

2.2. Synthesis of chalcone derivatives (**3a-3b**)

Compounds **3a** and **3b** were synthesized following a modified procedure based on the literature method.[4] A mixture of substituted acetophenone derivatives (**1a–b**, 1 mmol), benzaldehyde (**2**, 1 mmol), and 50% w/v aqueous KOH (1.2 mmol) in 15 mL of ethanol was stirred at room temperature for 3 hours. Upon completion of the reaction, the resulting solid was collected by vacuum filtration, washed with cold ethanol, and purified by recrystallization from ethanol.

*(E)-1,3-diphenylprop-2-en-1-one (**3a**)*

Yield: 98%. Yellow solid. IR (KBr pellet, cm^{-1}): 686, 774, 887, 1604, 1658, 3024, 3055. ^{1}H NMR ($CDCl_3$, 500 MHz) δ: 7.40-7.42 (m, 3H), 7.48-7.54 (m, 3H), 7.58 (t, *J* 7.3 Hz, 1H), 7.63-7.65 (m, 2H), 7.81 (d, *J* 15.7 Hz, 1H), 8.00-8.03 (m, 2H). ^{13}C NMR ($CDCl_3$, 125 MHz) δ: 122.3, 128.7, 128.7, 128.8, 129.2, 130.8, 133.0, 135.1, 138.4, 145.1, 190.8.

*(E)-1-(4-bromophenyl)-3-phenylprop-2-en-1-one (**3b**)*

Yield: 59%. Yellow solid. IR (KBr pellet, cm^{-1}): 817, 1072, 1396, 1481, 1597, 1658, 3055. ^{1}H NMR ($CDCl_3$, 500 MHz) δ: 7.49 (d, *J* 1.9 Hz, 2H), 7.50-7.52 (m, 4H), 7.53 (d, *J* 2.9 Hz, 2H), 7.73 (d, *J* 15.7 Hz, 1H), 8.00-8.02 (m, 2H). ^{13}C NMR ($CDCl_3$, 125 MHz) δ: 122.5, 124.8, 128.5, 128.7, 129.8, 132.2, 132.9, 133.8, 138.0, 143.4, 190.2.

2.3. Synthesis of 4,6-diarylpyrimidin-2(1*H*)-thiones derivatives (**5a-5b**)

Compounds **5a**-**5b** were synthesized using a previously reported protocol.[10] Substituted chalcones (**3a**-**3b**, 1 mmol), thiourea (**4**, 1 mmol), and KOH (1.7 mmol) were dissolved in 2.88 mL of ethanol and refluxed for 4 hours. Upon completion, the reaction mixture was poured onto crushed ice, and the resulting precipitate was collected by vacuum filtration and washed with cold ethanol. The crude products were purified by recrystallization from ethanol.

*4,6-diphenyl-3,4-dihydropyrimidine-2(1H)-thione (**5a**)*

Yield: 22%. Yellow solid. ^{1}H NMR (DMSO-d_6, 500 MHz) δ: 9.88 (s, 1H), 9.12 (s, 1H), 7.53 - 7.50 (m, 1H), 7.50 (d, *J* 1.8 Hz, 1H), 7.42 - 7.38 (m, 2H), 7.37 (dd, *J* 5.1, 1.9 Hz, 2H), 7.33 (dd, *J* 6.9, 4.3 Hz, 2H), 5.40 (dt, *J* 4.9, 1.6 Hz, 1H), 5.11 (dd, *J* 4.8, 2.8 Hz, 1H). ^{13}C NMR (DMSO-d_6, 125 MHz) δ: 54.6, 101.8, 122.0, 126.4, 127.6, 128.1, 128.7, 131.3, 132.5, 133.4, 143.9, 175.1.

*6-(4-bromophenyl)-4-phenyl-3,4-dihydropyrimidine-2(1H)-thione (**5b**)*

Yield: 51%. Yellow solid. ^{1}H NMR (DMSO-d_6, 500 MHz) δ: 9.95 (s, 1H), 9.13 (s, 1H), 7.58 - 7.54 (m, 2H), 7.47 - 7.44 (m, 2H), 7.39 (dd, *J* 10.3, 4.7 Hz, 2H), 7.31 (dt, *J* 9.1, 1.6 Hz, 3H), 5.43 (dd, *J* 3.3, 1.7 Hz, 1H), 5.11 (dd, *J* 4.9, 2.7 Hz, 1H). ^{13}C NMR (DMSO-d_6, 125 MHz) δ: 54.6, 101.8, 122.0, 126.4, 127.6, 128.1, 128.7, 131.3, 132.5, 133.4, 143.9, 175.1.

2.4. Chlorophyll a fluorescence measurement

Following a modified literature protocol,[16] ten spinach leaf disks (1.0 cm diameter) were placed in a 9 cm Petri dish containing 20 mL of modified Krebs solution. After an initial 12-hour incubation at room temperature, compounds **5a** and **5b** were added to the solution at a final concentration of 100 µM, using DMSO as the solvent, followed by an additional 6-hour incubation. Leaf disks were then dark-adapted for 30 minutes prior to measurement of chlorophyll *a* (Chl *a*) fluorescence transients using a Hansatech Handy Plant Efficiency Analyzer. Illumination was provided by a three-LED array emitting continuous red light at 650 nm. DMSO was used as the negative control to account for solvent effects, while 3-(3,4-dichlorophenyl)-1,1-dimethylurea (**DCMU**) was employed as a positive control. The OJIP fluorescence transients were analyzed using the JIP test methodology. All experiments were performed in triplicate, with results expressed as mean.

2.5. Molecular docking study

Molecular docking simulations were conducted, with modifications to a previously established protocol,[17] to evaluate the binding interactions of the enantiomers of compounds **5a** and **5b** with the active site of the D1 protein in photosystem II (PSII). The ligand structures were drawn using ChemDraw Professional 15.0[18] and subjected to geometry optimization through MM2 energy minimization. The three-dimensional structure of the D1 protein (PDB ID: 4V82) was obtained from the Protein Data Bank. Prior to docking, all water molecules and co-factors were removed, polar hydrogens were added, and atomic charges were assigned using the Gasteiger method in AutoDockTools (ADT).[19]

Docking simulations were performed using both AutoDock Vina[20] and AutoDock 4.2.[21] The protein structure was converted to pdbqt format, and docking parameters were specified via a config.txt file for Vina. For AutoDock 4.2., a grid box of 40 × 40 × 40 points with a spacing of 0.286 Å was defined, centered at coordinates x = 21.804, y = 67.331, and z = 34.939, corresponding to the PSII binding site. Each simulation was run independently 20 times. The best binding poses were selected based on their interaction with key amino acid residues, number of hydrogen bonds, and the lowest binding energy values. Intermolecular interactions were analyzed using BIOVIA Discovery Studio 2024,[22] and molecular visualizations were rendered with PyMOL.[23]

3. Results and Discussion

3.1. Synthesis and characterization of 4,6-diarylpyrimidin-2(1*H*)-thiones derivatives (**5a-5b**)

Chalcones **3a**-**3b** were synthesized in excellent yields via a Claisen–Schmidt aldol condensation using substituted acetophenones (**1a**-**3b**), benzaldehyde (**2**), potassium hydroxide as a base catalyst, and ethanol as the reaction medium (Scheme 1).

The 4,6-diarylpyrimidin-2(1*H*)-thione derivatives (**5a** and **5b**) were synthesized via a condensation reaction between the chalcones **3a** and **3b** and thiourea, using potassium hydroxide as a base in ethanol under reflux (Scheme 2). The reactions were carried out under reflux for 4 hours, affording the desired compounds **5a** and **5b** in moderate yields after recrystallization.

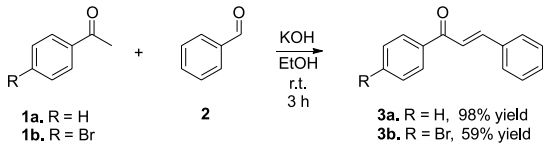

Scheme 1. Synthesis of chalcones **3a**-**3b**

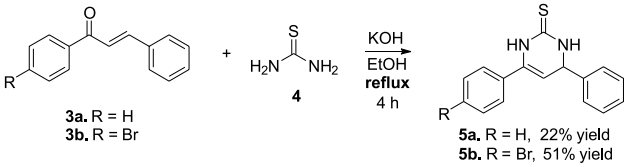

Scheme 2. Synthesis of 4,6-diarylpyrimidin-2(1*H*)-thione derivatives **5a** and **5b**

All synthesized compounds were characterized by ^{1}H and ^{13}C NMR spectroscopy, and the spectral data were consistent with previously reported literature.[24,25] In the ^{1}H NMR spectra, the NH protons appeared as distinct singlets in the range of 9.95 to 9.12 ppm. The ^{13}C NMR spectra exhibited a characteristic signal at 175.1 ppm, attributed to the carbon of the thiourea moiety. Additionally, the ^{1}H NMR spectra revealed the presence of vicinal protons on the pyrimidin-2(1*H*)-thione ring, appearing as two doublets of doublets, each integrating for one proton, with coupling constants of 4.9 and 1.8 Hz. These were observed at 5.40–5.43 ppm and 5.11 ppm, respectively. The aromatic region displayed signals consistent with the aryl substituents attached to the pyrimidin-2(1*H*)-thione ring, further confirming the structure of the synthesized derivatives.

The chalcone molecule adopts a planar conformation due to extended conjugation between its aromatic rings, the α,β-unsaturated double bond, and the carbonyl group. This delocalization confers structural rigidity and establishes a mirror plane that divides the molecule into distinct upper and lower faces. During the reaction, thiourea acts as

a nucleophile, attacking the electrophilic carbon of the chalcone's carbonyl group. Owing to the planarity of the substrate, the nucleophilic attack by thiourea can occur from either face of the molecule (Scheme 3).

An attack from the upper face leads to the formation of the *R* enantiomer, whereas attack from the lower face results in the *S* enantiomer. This nucleophilic addition disrupts the planarity and introduces a new stereocenter at the former carbonyl carbon. In the absence of any chiral catalyst, the reaction proceeds with equal probability from both faces, leading to the formation of a racemic mixture comprising both enantiomers in a 1:1 ratio.[26]

3.2. Chl *a* fluorescence assay

To elucidate the mode of action of compounds **5a** and **5b**, their effects on Chl *a* fluorescence parameters were compared with the well-known PSII inhibitor **DCMU**. The radar plot illustrates the effects of 4,6-diarylpyrimidin-2(1*H*)-thione derivatives and **DCMU** on photosynthetic performance, based on Chl *a* fluorescence parameters. These measurements provide insights into the efficiency and functionality of PSII under compound exposure, with untreated plants (control) normalized to a reference value of 1.0 (Figure 1).

Compounds **5a** and **5b** reduced the performance index on an absorption basis ($\mathbf{PI_{abs}}$) by 74% and 65%, respectively, compared to the control group. Additionally, both compounds altered key parameters associated with PSII reaction centers (RCs), including energy fluxes for light absorption (**ABS/RC**), excitation energy trapping ($\mathbf{TR_0/RC}$), electron transport ($\mathbf{ET_0/RC}$), and energy dissipation ($\mathbf{DI_0/RC}$), as well as quantum yield indicators ($\mathbf{PHI(P_0)}$, $\mathbf{PSI_0}$ and $\mathbf{PHI(E_0)}$). These changes reinforce the inhibitory effect of the compounds on PSII function (Figure 1).[27]

Compound **5a** reduced $\mathbf{ET_0/RC}$, $\mathbf{PSI_0}$ and $\mathbf{PHI(E_0)}$ by 17%, 18%, and 22%, respectively (Figure 1 – Chart **A**), indicating a disruption in electron flow through the photosynthetic electron transport chain. This suggests that functional PSII reaction centers were transformed into inactive or energy-dissipating units due to impaired reduction of the primary quinone acceptor Q_A.[28] Compound **5b** produced a comparable effect, with decreases of 30%, 16%, and 20% in $\mathbf{ET_0/RC}$, $\mathbf{PSI_0}$ and $\mathbf{PHI(E_0)}$, respectively (Figure 1 – Chart **B**), implying that a greater proportion of absorbed energy was retained and diverted away from photochemistry, thereby limiting electron transport through active RCs. The involvement

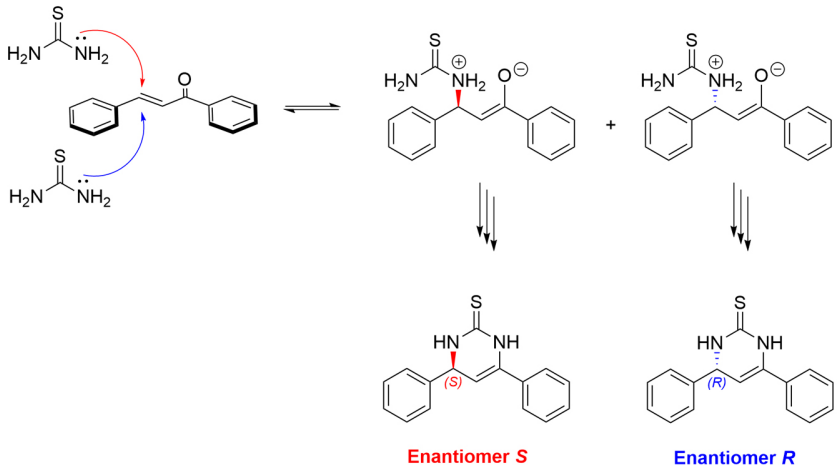

Scheme 3. Schematic representation of thiourea nucleophilic attack on the two non-equivalent faces of the α,β-unsaturated carbonyl double bond, resulting in racemic compound **5a**

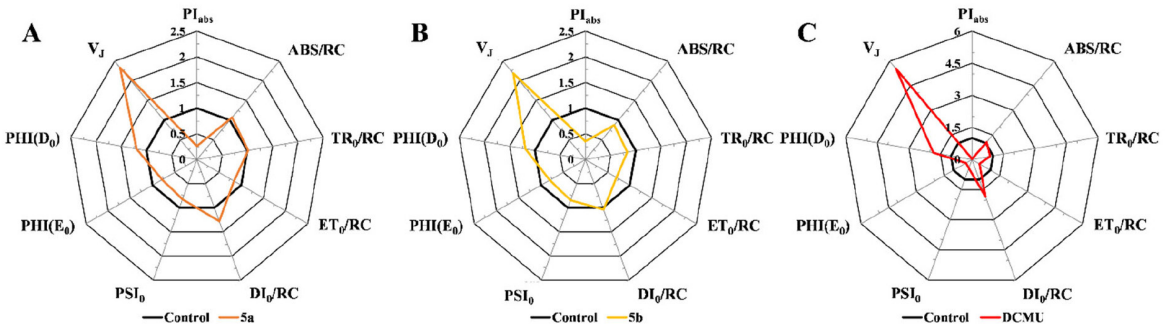

Figure 1. Radar plots of the effects of compounds **5a** (Chart - **A**), **5b** (Chart - **B**) and **DCMU** (Chart - **C**) on Chl *a* fluorescence parameters calculated from the OJIP curve in *S. oleracea* leaf disks at 100 µM

of the PsbS protein, known to mediate non-photochemical quenching, may contribute to enhanced energy dissipation as heat under these stress conditions.[29] Furthermore, both compounds increased the $\mathbf{V_J}$ parameter by 133% for **5a** and 118% for **5b**. This increase in fluorescence at the J-step of the OJIP transient is indicative of impaired electron transport beyond Q_A, supporting the hypothesis that these compounds inhibit Q_A reoxidation by restricting electron flow toward Q_B in the quinone pool.[30]

Although **DCMU** exhibited a stronger inhibitory effect on $\mathbf{PI_{abs}}$, $\mathbf{V_J}$, $\mathbf{ET_0/RC}$ and $\mathbf{PSI_0}$ (Figure 1 – Chart **C**), compounds **5a** and **5b** caused comparatively milder reductions in these parameters. Both compounds also induced moderate increases in **ABS/RC** and $\mathbf{TR_0/RC}$, likely reflecting a compensatory accumulation of excitation energy at the reaction centers due to hindered electron transport beyond Q_A.[31] These observations suggest that, although compounds **5a** and **5b** may act via a mechanism similar to that of **DCMU**, their interaction with the PSII complex may involve distinct binding characteristics or reduced affinity. These data support the conclusion that compounds **5a** and **5b** disrupt photosynthetic electron flow in a manner analogous to **DCMU**, reinforcing their potential as PSII-targeting herbicidal agents. To further rationalize these physiological findings at the molecular level, docking simulations were performed to explore the binding interactions of both enantiomers with the Q_B-binding niche of the D1 protein.

3.3. Molecular docking

The docking simulations provided insights into the binding interactions and potential inhibitory mechanisms of the synthesized pyrimidin-2(1*H*)-thione derivatives with the D1 protein of PSII. By correlating these *in silico* results with the chlorophyll fluorescence data, it becomes evident that the strong hydrogen bonding and hydrophobic contacts predicted for the S-enantiomers are consistent with the observed impairment of Q_A to Q_B electron transport. This complementary evidence reinforces the mechanistic hypothesis that the inhibitory effects detected in vivo arise from the stereoselective binding of the compounds within the Q_B pocket.

For compound **5a**, although both enantiomers displayed comparable binding energies (-8.6 kcal/mol), the *S*-form engaged in a more effective binding pose, forming a key hydrogen bond with His215 and π–π stacking interactions with Phe255, complemented by hydrophobic contacts with Leu218, Leu271, and Ala251. This combination of interactions suggests that the stereochemistry of the chiral center governs not only ligand orientation but also the alignment of pharmacophoric groups within the binding pocket (Figure 2).

Similarly, the *S*-enantiomer of compound **5b** demonstrated a slightly superior binding affinity (−8.3 kcal/mol) compared to its *R*-enantiomer. The enhanced binding of the S-enantiomer was attributed to a strong hydrogen bond with His215 and multiple hydrophobic interactions with key residues (Leu218, Leu271, Ala251, and Phe265), as well as π–π stacking with Phe265. These interactions underscore the importance of the C=S functional group in mediating specific protein–ligand recognition events (Figure 3).

Commercial herbicides, such as diuron, bind to the His215, Ser264, and Phe265 residues of PSII. Similarly, compounds **5a** and **5b** adopted the same orientation within the D1 protein binding pocket. Notably, diuron forms a hydrogen bond between its carbonyl group and NH backbone of the His215 residue.[14] Additionally, the docking results were consistent with experimental data on Chl *a* fluorescence inhibition, in which compounds bearing electron-rich aromatic substituents and planar heterocyclic cores exhibited significant disruption of PSII function. The correlation between binding affinity and biological activity

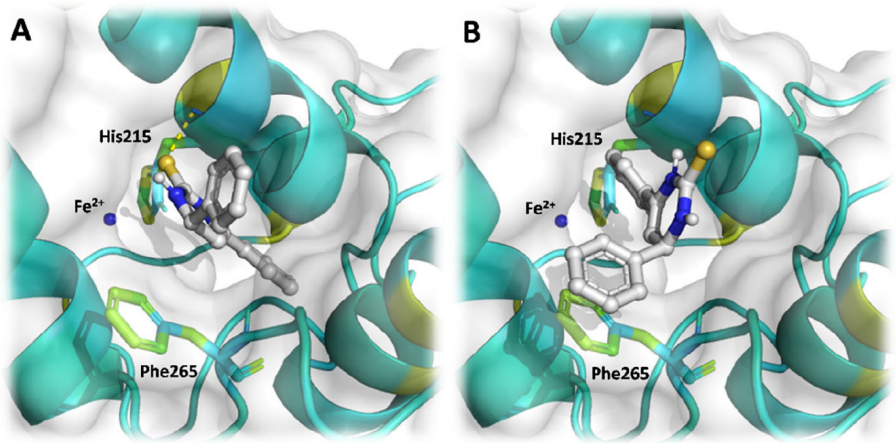

Figure 2. Binding modes for compound **5a**: *S*-enantiomer (Chart - **A**) and *R*-enantiomer (Chart - **B**)

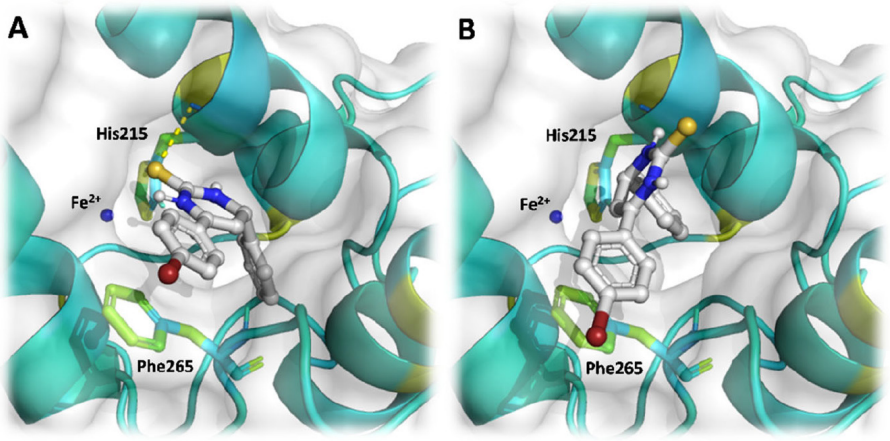

Figure 3. Binding modes for compound **5b**: *S*-enantiomer (Chart - **A**) and *R*-enantiomer (Chart - **B**)

suggests that structural features promoting hydrophobic embedding and hydrogen bonding capacity enhance PSII inhibition. Together, the experimental and computational data converge on the same mechanism: stereochemistry-dependent binding of the 4,6-diarylpyrimidin-2(1*H*)-thione derivatives to the D1 protein, leading to impaired electron flow through PSII. Overall, the molecular docking analysis supports the hypothesis that the spatial arrangement of substituents, stereochemistry, and electron-donating/withdrawing character of the aryl groups play critical roles in defining the herbicidal potential of the compounds.

4. Conclusion

We synthesized two 4,6-diarylpyrimidin-2(1*H*)-thione derivatives and confirmed their potential as PSII inhibitors. Compound **5a** exhibited strong herbicidal activity, both in chlorophyll fluorescence assays and *in silico*, highlighting its capacity to bind effectively to the D1 protein. The docking studies revealed that both the spatial orientation and the nature of aromatic substituents are crucial for inhibitory activity. These findings support the development of 4,6-diarylpyrimidin-2(1*H*)-thione derivatives as promising leads for next-generation herbicides targeting PSII.

Supplementary Information

Supplementary information are available free of charge at https://rvq.sbq.org.br/pdf/AR2026-5041-MS.

Acknowledgments

The authors express their appreciation to CNPq (grant 420048/2023-5) and UFMT for financial support and fellowships. This study was financed in part by the Coordenação de Aperfeiçoamento de Pessoal de Nível Superior - Brasil (CAPES) - Finance Code 001.

Authors Contribution

Lucas C. C. Vieira: Project administration, Conceptualisation, Writing – original draft, Writing – review and editing; Kettlyn A. R. T. Santos: Research; Taciane S. Pitteri: Research, Writing – original draft; Raquel S. Garralda: Research; Marcelo A. F. Basso: Research; Leonardo G de Vasconcelos: Data curation; Olívia M. Sampaio: Data curation.

Bibliographic References

1. Berestetskiy, A.; Modern Approaches for the Development of New Herbicides Based on Natural Compounds. *Plants* **2023**, *12*, 234. [Crossref] [PubMed]
2. Li, J.; Zhang, Z.; Lei, Q.; Lu, B.; Jin, C.; Liu, X.; Wang, Y.; Bai, L.; Multiple herbicide resistance in *Eleusine indica* from sugarcane fields in China. *Pesticide Biochemistry and Physiology* **2022**, *182*, 105040. [Crossref] [PubMed]
3. Basappa, V. C.; Ramaiah, S.; Penubolu, S.; Kariyappa, A. K.; Recent Developments on the Synthetic and Biological Applications of Chalcones-A Review. *Biointerface Research in Applied Chemistry* **2022**, *12*, 180. [Crossref]
4. Bandeira, P. N.; Fontenele, R. O. S.; Costa, P. S.; Santos, H. S.; de Lemos, T. L. G.; *In Vitro* Antifungal Activity Against *Trychophyton Rubrum* of *p*-Aminochalcones and 3'-Methoxy-4'-Hydroxy Chalcone. *Revista Virtual de Química* **2020**, *12*, 703. [Crossref]
5. Vásquez-Martínez, Y. A.; Osorio, M. E.; San Martín, D. A.; Carvajal, M. A.; Vergara, A. P.; Sanchez, E.; Raimondi, M.; Zacchino, S. A.; Mascayano, C.; Torrent, C.; Cabezas, F.; Mejias, S.; Montoya, M.; Cortez-San Martín, M.; Antimicrobial, Anti-Inflammatory and Antioxidant Activities of Polyoxygenated Chalcones. *Journal of the Brazilian Chemical Society* **2019**, *30*, 286. [Crossref]
6. Gao, F.; Huang, G.; Xiao, J.; Chalcone hybrids as potential anticancer agents: Current development, mechanism of action,

and structure-activity relationship. *Medicinal Research Reviews* **2020**, *40*, 2049. [Crossref]

7. de Pádua, G. M. S.; Pitteri, T. S.; Basso, M. A. F.; de Vasconcelos, L. G.; Ali, A.; Dall'Oglio, E. L.; Sampaio, O. M.; Vieira, L. C. C.; Synthesis and Evaluation of New Phytotoxic Fluorinated Chalcones as Photosystem II and Seedling Growth Inhibitors. *Chemistry & Biodiversity* **2024**, *21*, e202301564. [Crossref] [PubMed]
8. Amslinger, S.; The Tunable Functionality of α,β-Unsaturated Carbonyl Compounds Enables Their Differential Application in Biological Systems. *ChemMedChem* **2010**, *5*, 351. [Crossref] [PubMed]
9. Vdovina, S. V; Mamedov, V. A. O.; New potential of the classical Biginelli reaction. *Russian Chemical Reviews* **2008**, *77*, 1017. [Crossref]
10. Kodhati, V.; Vanga, M. R.; Yellu, N. R.; Synthesis and Anti Bacterial and Anti-ulcer Evaluation of New S-mannich Bases of 4,6-diaryl-3,4-dihydropyrimidin-2(1*H*)-thiones. *Journal of the Korean Chemical Society* **2013**, *57*, 234. [Crossref]
11. Mustafa, M.; Winum, J.-Y.; The importance of sulfur-containing motifs in drug design and discovery. *Expert Opinion on Drug Discovery* **2022**, *17*, 501. [Crossref] [PubMed]
12. Kojasoy, V.; Tantillo, D. J.; Impacts of noncovalent interactions involving sulfur atoms on protein stability, structure, folding, and bioactivity. *Organic & Biomolecular Chemistry* **2023**, *21*, 11. [Crossref] [PubMed]
13. Didaran, F.; Kordrostami, M.; Ghasemi-Soloklui, A. A.; Pashkovskiy, P.; Kreslavski, V.; Kuznetsov, V.; Allakhverdiev, S. I.; The mechanisms of photoinhibition and repair in plants under high light conditions and interplay with abiotic stressors. *Journal of Photochemistry and Photobiology B: Biology* **2024**, *259*, 113004. [Crossref] [PubMed]
14. Battaglino, B.; Grinzato, A.; Pagliano, C.; Binding Properties of Photosynthetic Herbicides with the Q_B Site of the D1 Protein in Plant Photosystem II: A Combined Functional and Molecular Docking Study. *Plants* **2021**, *10*, 1501. [Crossref] [PubMed]
15. Yu, X.; Chen, Z.; Lv, L.; Li, M.; Li, Q.; Evaluation of Chiral Pesticide Chlorbufam at the Enantiomeric Level: Absolute Configuration, Separation, Herbicidal Activity, and Degradation in Soil. *Journal of Agricultural and Food Chemistry* **2025**, *73*, 5748. [Crossref] [PubMed]
16. Moura, M. S.; Lacerda, J. W. F.; Siqueira, K. A.; Bellete, B. S.; Sousa Jr., P. T.; Dall´Óglio, E. L.; Soares, M. A.; Vieira, L. C. C.; Sampaio, O. M.; Endophytic fungal extracts: evaluation as photosynthesis and weed growth inhibitors. *Journal of Environmental Science and Health, Part B* **2020**, *55*, 470. [Crossref] [PubMed]
17. de Souza, J. M.; Medeiros, P. S.; Pitteri, T. S.; Silva, M. A.; Basso, M. A. F.; de Vasconcelos, L. G.; Dall'Óglio, E. L.; Sampaio, O. M.; Vieira, L. C. C.; Acridone Derivatives as Photosystem II Inhibitors: Synthesis, Herbicidal Activity, and Structure-Activity. *Journal of the Brazilian Chemical Society* **2025**, 36, e-20240224. [Crossref]
18. *ChemDraw*, version 19.0; PerkinElmer Informatics, Inc.; CambridgeSoft, USA, **2019**.
19. *AutoDockTools*, version 1.5.7; The Scripps Research Institute, USA, **2022**.
20. *AutoDock Vina*, version 1.2.5; The Scripps Research Institute, USA, **2024**.
21. *AutoDock*, version 4.2.6; The Scripps Research Institute, USA, **2022**.
22. *Discovery Studio Visualizer*, version 21.1.0.20298; Biovia, USA, **2012**.
23. *The PyMOL Molecular Graphics System*, version 2.1.0; Schrödinger, LLC., USA, **2018**.
24. Grechanik, V.; Romanova, A.; Naydov, I.; Tsygankov, A.; Photoautotrophic cultures of *Chlamydomonas reinhardtii*: sulfur deficiency, anoxia, and hydrogen production. *Photosynthesis Research* **2020**, *143*, 275. [Crossref] [PubMed]
25. Ni, L.; Acharya, K.; Hao, X.; Li, S.; Li, Y.; Li, Y.; Effects of Artemisinin on Photosystem II Performance of *Microcystis aeruginosa* by *In Vivo* Chlorophyll Fluorescence. *Bulletin of Environmental Contamination and Toxicology* **2012**, *89*, 1165. [Crossref] [PubMed]
26. De Souza, J. M.; Fazolo, B. R.; Lacerda, J. W. F.; Moura, M. S.; dos Santos, A. C. R.; de Vasconcelos, L. G.; de Sousa Junior, P. T.; Dall'Oglio, E. L.; Ali, A.; Sampaio, O. M.; Vieira, L. C. C.; Rational Design, Synthesis and Evaluation of Indole Nitrogen Hybrids as Photosystem II Inhibitors. *Photochemistry and Photobiology* **2020**, *96*, 1233. [Crossref] [PubMed]
27. Zhang, B.; Zhang, H.; Jing, Q.; Wang, J.; Light pollution on the growth, physiology and chlorophyll fluorescence response of landscape plant perennial ryegrass (*Lolium perenne L.*). *Ecological Indicators* **2020**, *115*, 106448. [Crossref]
28. Chen, H.; Song, L.; Zhang, H.; Wang, J.; Wang, Y.; Zhang, H.; Cu and Zn Stress affect the photosynthetic and antioxidative systems of alfalfa (*Medicago sativa*). *Journal of Plant Interactions* **2022**, *17*, 695. [Crossref]